

MAPAN-JOURNAL ,
Publisher: METROLOGY SOC INDIA , NPL PREMISES,
Address: DR K S KRISHNAN MARG, NEW DELHI, INDIA,
ISSN / eISSN:0970-3950 / 0974-9853
Volume 25-Issue 1-(2025)
https://doi-001.org/1025/17617210929207



# STUDY OF THE EARTHING OF AN ELECTRICAL INSTALLATION— CIRCUITAL APPROACH, FDTD AND FIT MODELLING (a) Check for updates

Mohammed Kaouka<sup>1</sup>, Hakim Azizi <sup>2</sup>, Adelhadi Hameurlaine <sup>1</sup>, Mohammed Chebout <sup>1</sup>, Mohammed Charif Kihal <sup>3</sup>, Daoud Sekki <sup>4</sup> and Marouane Kihal <sup>5</sup>

<sup>1</sup> Applied Automation and industrial Diagnostic Laboratory, Ziane achour university, Djelfa, Algeria.

<sup>2</sup> Renewable Energy Systems Applications Laboratory, Ziane achour university, Djelfa, Algeria.
 <sup>3</sup> L2EI Laboratory, Mohamed Seddik Ben Yahia University, Jijel, Algeria.
 <sup>4</sup> Faculty of technology Mohamed Cherif Messaadia University - Souk Ahras, Algeria.
 <sup>5</sup> Faculty of Exact Sciences, Bejaia University, Bejaia, Algeria.

Email: mohammed.kaouka@ univ-djelfa.dz

Received: 13/03/2025; Accepted: 28/09/2025

#### Abstract

In this work, we detail the resolution of Maxwell's equations in 3D by the numerical method called FDTD (Finite Difference Time Domain) for a homogeneous or horizontally stratified soil in the presence of an earthing that we count as first contribution, then we propose a new way based on the use of the concept of transmission lines associated with topological formalism, which we consider to be simpler and more realistic in terms of mathematical model, allowing a modeling as well in frequency (taking into account the effect of frequency on resistivity) only in time (taking into account non-linearity) with a very reduced calculation time.

To validate our work, we compared our calculation results by means of transmission line equations by  $matrix[\emptyset]$  (TL-  $matrix[\emptyset]$ ) with those obtained by solving the maxwell equations by FDTD in the case of laminate floors where we introduce the notion of apparent resistivity as well as with those obtained by software of simulation CST Software.

**Keywords:** The earthing, Maxwell's equations, FDTD, CST Software, Transmission line,

#### I. INTRODUCTION

The grounding of an electrical installation consists in connecting the masses or the neutral of the installation to a ground connection via one or more earth conductors. In the stations of the energy transmission network, this grounding of masses and neutral is common [1]. The earthing plug, called earth grid for major installations such as substations, consists of a set of buried conductors in direct contact with the ground and electrically connected to each other. Its role is to allow the flow, inside the soil, of fault currents of all origins. During such flows through the earth network, potential differences may appear between certain points, for example between two metal masses, between a metal mass and the ground, or between two points on the ground. The design of the earth grid must

allow, even under these conditions, to ensure the maintenance, protection of power installations, protection of sensitive equipment and a reference potential [2-5]

When making an earthing, the parameters to be taken into account at the outset are the resistivity of the ground, the dimensions of the ground to make the earth network, the intensity of the fault current and the duration of the fault. The cost of implementation factor will also be integrated during the study to compare different possible solutions [6].

Seasonal climatic variations affect the resistivity of the surface layers of a land. Also, soil resistivity measurements can be complicated by the presence of metallic bodies in the prospected area. These disadvantages require the repetition (depending on climatic conditions and at several nearby points) of the in situ measurement to characterize an earthing (resistance measurement) [7-9].

In order to characterize grounding, it is advantageous to know its transient impedance (also called impulse resistance). The transient impedance is defined by the graph Z(t)=U(t)/I(t) corresponding to a given current wave or sometimes more summarily, as the minimum value of Z(t), or as the value of Z(t) at the time of the maximum of U(t). In all cases, the transient impedance depends on different parameters (spectral content and current amplitude, soil resistivity, grounding shape, non-linearity...). In principle, the complete specification of a ground plug therefore requires data from a series of Z(t) graphs [10].

In view of the various parameters which condition the transient behaviour of a ground plug, analysis by repetition alone of the measurement proved to be insufficient and very expensive [11, 12].

To overcome this difficulty, analytical methods for simple geometries have been developed and several computer numerical calculation methods have been established by various authors. These methods are primarily applied in practice to the design of ground networks for large installations (e.g. large substations) [13-17].

### II. ELECTROMAGNETIC MODELING OF AN EARTHING

# II.1. FDTD RESOLUTION OF MAXWELL'S EQUATIONS

In this part, we devote it to the modeling of the transient behavior of an earthing by numerical resolution of Maxwell's equations (Maxwell-Ampère and Maxwell-Faraday); the numerical method used is the so-called FDTD (Finite Difference Time Domain). We briefly discuss Maxwell's general equations and recall the principle of the so-called FDTD numerical method [18-22].

We then present the discretization by FDTD of the Maxwell-Ampère and Maxwell-Faraday equations, in an infinite medium, developed on the basis of the concept of the Yee [23] and we briefly recall the different notions used to take into account open boundaries.

To extend this concept to the modeling of an earthing, we detail the mathematical writings of the earth conductors, the consideration of the ground-air interface as well as that of open boundaries. Also, in order to take into account the horizontal stratification of the soil we extend the concept called "Contour Integral Approach" to the interface between two soil layers of different conductivities [24].

#### II.1.1. PRINCIPE OF THE METHOD

Let us take f(x), a continuous and differentiable function, it is possible to obtain an approximation for the derivative at the point  $x_0$ , based on the Taylor series expansion: the Taylor series expansion of the right differentiation is given by [18]:

$$f\left(x_0 + \frac{\Delta x}{2}\right) = f(x_0) + \frac{\Delta x}{2}f'(x_0) + \frac{\Delta x^2}{8}f''(x_0) + \cdots$$
 (1)

$$f\left(x_0 - \frac{\Delta x}{2}\right) = f(x_0) - \frac{\Delta x}{2}f'(x_0) + \frac{\Delta x^2}{8}f''(x_0) - \cdots$$
 (2)

Now we subtract these two equations (1) and (2) and divide the result by  $\Delta x$ , which gives us the following result:

$$f'(x_0) = \frac{f\left(x_0 + \frac{\Delta x}{2}\right) - f\left(x_0 - \frac{\Delta x}{2}\right)}{\Delta x} + \theta(\Delta x^2)$$
(3)

With:

 $\theta(h^2)$ : represents the second-order error committed, which will be neglected subsequently.

This approximation of the derivative is called a centered approximation. The results it provides are more precise in comparison with those given by other types of so-called right or left approximations, whose expressions (4) and (5) are described respectively below:

$$f'(x_0) = \frac{f(x_0) - f\left(x_0 - \frac{\Delta x}{2}\right)}{\Delta x} + \theta(\Delta x) \tag{4}$$

$$f'(x_0) = \frac{f\left(x_0 + \frac{\Delta x}{2}\right) - f(x_0)}{\Delta x} + \theta(\Delta x) \tag{5}$$

It is noted that the term  $\theta(\Delta x)$  which is of the first order is less precise in comparison with that of the second order of the centered derivative. Therefore, we will use the centered approximation in our study to discretize the partial, spatial and temporal derivatives present in Maxwell's equations [18-20]. We calculate the centered derivative of a function (figure.1) at the center of an interval based on the values of the function at the ends.

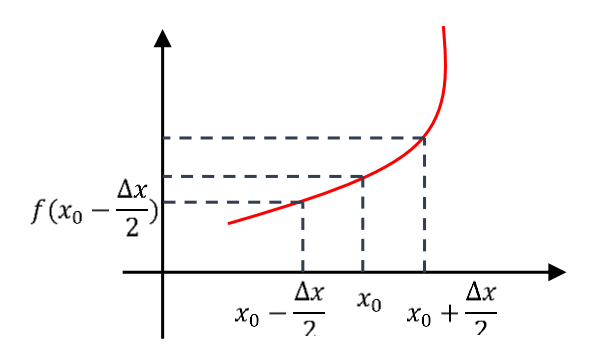


Figure 1: Calculation point of the centered derivative. Source: Authors (Andrieuet al .1999)

In electromagnetism, this approximation technique can be applied to the wave equation (in the frequency or time domain), to rotational equations (in the time domain) or to global forms (Maxwell-Faraday and Maxwell-Ampère equations, in both domains). Consequently, Maxwell's equations (4) and (5) will be expressed on each interval from this approximation. It can be noted that the spatial derivatives are linked to the temporal derivatives. They will each be the subject of a particular discretization, either with respect to space or with respect to time [20].

### II.1.2. DISCRETIZATION OF MAXWELL'S EQUATIONS BY FDTD

Given the two Maxwell equations (5) and (6), in a non-magnetic conducting medium (absence of magnetization current), we have in the absence of an excitation current [21]:

$$\overrightarrow{rot}\vec{E} = -\frac{\partial \vec{B}}{\partial t} \tag{5}$$

$$\overrightarrow{rot}\overrightarrow{H} = \frac{\partial \overrightarrow{D}}{\partial t} + \overrightarrow{J}_c \tag{6}$$

With:

$$\vec{J}_c = \sigma \vec{E}$$

For the first three equations, the starting point is the Maxwell-Faraday equation (5). We recall that we have for each of the components B of  $\vec{B}$ :  $B = \mu H$ 

Expressed in a Cartesian coordinate system, the three scalar equations that arise from the Maxwell-Faraday rotational equation (5), in a homogeneous and isotropic linear medium characterized by  $\varepsilon$ ,  $\mu$  and  $\sigma$  in the absence of charge density and excitation current, are [21]:

$$\frac{\partial H_x}{\partial t} = \frac{1}{\mu} \left( \frac{\partial E_y}{\partial z} - \frac{\partial E_z}{\partial y} \right) \tag{7}$$

$$\frac{\partial H_y}{\partial t} = \frac{1}{\mu} \left( \frac{\partial E_z}{\partial x} - \frac{\partial E_x}{\partial z} \right) \tag{8}$$

$$\frac{\partial H_z}{\partial t} = \frac{1}{\mu} \left( \frac{\partial E_x}{\partial y} - \frac{\partial E_y}{\partial x} \right) \tag{9}$$

For the other three scalar equations, we use the Maxwell-Ampère law (6), which links the fields  $\vec{B}$  and  $\vec{E}$  by involving the current density vector  $\vec{J_c}$  [21].

$$\frac{\partial E_x}{\partial t} = \frac{1}{\varepsilon} \left( \frac{\partial H_z}{\partial y} - \frac{\partial H_y}{\partial z} - \sigma E_x \right) \tag{10}$$

$$\frac{\partial E_y}{\partial t} = \frac{1}{\varepsilon} \left( \frac{\partial H_x}{\partial z} - \frac{\partial H_z}{\partial x} - \sigma E_y \right) \tag{11}$$

$$\frac{\partial E_z}{\partial t} = \frac{1}{\varepsilon} \left( \frac{\partial H_y}{\partial x} - \frac{\partial H_x}{\partial y} - \sigma E_z \right)$$
 (12)

Each of the partial derivatives, of the first order, can be expressed by a finite-centered difference as explained in paragraph (5):

$$\frac{\Delta F}{\Delta v} = \frac{1}{\Delta v} \left( f \left( v + \frac{\Delta v}{2} \right) - f \left( v - \frac{\Delta v}{2} \right) \right) \tag{13}$$

Where represents one of the variables x, y, z and t, and F represents any of the components of the electromagnetic field expressed in Cartesian coordinates.

To each node of the mesh thus defined, we can associate a triplet of integers (i,j,k) such that the coordinates  $(x_i,y_j,z_k)$  of the node verify the following relation:  $x_i=i\Delta x$ ;  $y_j=j\Delta y$ ;  $z_k=k\Delta z$ 

Thus, if F represents one of the field components, we will subsequently adopt the following notation:

$$F^{n}(i,j,k) = F(i\Delta x, j\Delta y, k\Delta z, n\Delta t)$$
 (14)

By convention, the index n corresponding to the time discretization is put in exponent of the field component F. The components of the electromagnetic field are located at different points in an elementary mesh. Indeed, the electric components are calculated according to the edges and the magnetic components normally to the faces.

#### II.1.2. TIME AND SPACE SAMPLING

The components of the electromagnetic field are located at different points in an elementary mesh (figure .2). Indeed, the electric components are calculated according to the edges and the magnetic components normally to the faces [23].

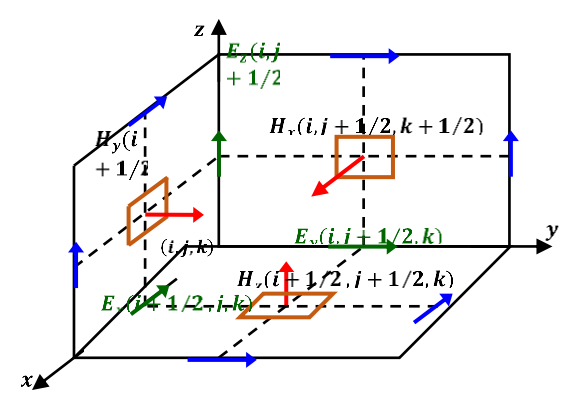


Figure 2: Yee elementary cell. Source: Authors (2025)

Using the notation (14) to express equation (5) under the approximation (13), we obtain:

$$\frac{H_x^{n+\frac{1}{2}}\left(i,j+\frac{1}{2},k+\frac{1}{2}\right)-H_x^{n-\frac{1}{2}}\left(i,j+\frac{1}{2},k+\frac{1}{2}\right)}{\Delta t} = \frac{1}{\mu} \begin{bmatrix} E_y^n\left(i,j+\frac{1}{2},k+1\right)-E_y^n\left(i,j+\frac{1}{2},k\right)\\ \Delta z\\ -\frac{E_z^n\left(i,j+1,k+\frac{1}{2}\right)-E_z^n\left(i,j,k+\frac{1}{2}\right)}{\Delta y} \end{bmatrix}$$
(15)

From equations of type (15), we can establish an algorithm for calculating the scalar components of the electromagnetic field that proceeds by incrementing the discrete spatial and temporal values. This procedure is known as "leapfrog" and was initially proposed by K. Yee in [23]. We observe that the value of the component  $H_x$  at time  $\left(n + \frac{1}{2}\right)\Delta t$  can be expressed as a function of the value of this same component at the previous time step, and of the values of the components  $E_y$  and  $E_z$  at the half-previous time step. We can therefore, by making the hypothesis (non-restrictive, and for the example) of a cubic mesh of side  $\Delta l$ , explicitly express the future value of  $H_x$  as a function of known values:

$$H_{x}^{n+\frac{1}{2}}\left(i,j+\frac{1}{2},k+\frac{1}{2}\right) = H_{x}^{n-\frac{1}{2}}\left(i,j+\frac{1}{2},k+\frac{1}{2}\right) + \frac{\Delta t}{\mu\Delta l} \begin{bmatrix} E_{y}^{n}\left(i,j+\frac{1}{2},k+1\right) - E_{y}^{n}\left(i,j+\frac{1}{2},k\right) \\ + E_{z}^{n}\left(i,j,k+\frac{1}{2}\right) - E_{z}^{n}\left(i,j+1,k+\frac{1}{2}\right) \end{bmatrix}$$
(16)

Similarly, reasoning in the xOz plane, the component  $E_y$  at time  $(n+1)\Delta t$  is expressed as the linear combination of the components  $H_x$  and  $H_z$  at time  $(n+1/2)\Delta t$  and of the component  $E_y$  at time  $n\Delta t$ :

$$E_y^{n+1}\left(i,j\frac{1}{2},k\right)\left(\frac{\varepsilon/\Delta t-\sigma/2}{\varepsilon/\Delta t+\sigma/2}\right).E_y^n\left(i,j\frac{1}{2},k\right)\frac{1}{(\varepsilon/\Delta t+\sigma/2)\Delta l}*$$

$$\begin{bmatrix} H_x^{n+\frac{1}{2}} \left( i, j + \frac{1}{2}, k + \frac{1}{2} \right) - H_x^{n+\frac{1}{2}} \left( i, j + \frac{1}{2}, k - \frac{1}{2} \right) \\ + H_z^{n+\frac{1}{2}} \left( i - \frac{1}{2}, j + \frac{1}{2}, k \right) - H_z^{n+\frac{1}{2}} \left( i + \frac{1}{2}, j + \frac{1}{2}, k \right) \end{bmatrix}$$
(17)

#### II.1.4. APPLICATION OF THE FDTD METHOD TO THE MODELING OF EARTHING

K. Tanabe [25] has already addressed the problem of earthing by solving Maxwell's equations by FDTD; in his work the author only deals with the case of a simple conductive square loop buried in a homogeneous soil. Inspired by this first work, we propose some additional elements for the analysis of the transient behavior of a real-size earthing grid (equipping an electrical substation) taking into account the horizontal stratification of the soil and open boundaries (figure. 3).

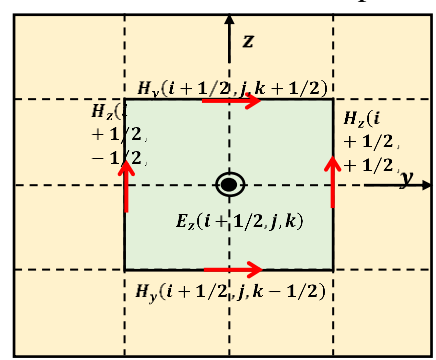


Figure 3: Arrangement of the components of the magnetic field around the thin conductor. Source: Authors (2025)

We obtain the following magnetic field equation and electric field equation:

$$H_{z}^{n+\frac{1}{2}}(i+1/2,j+1/2,k)$$

$$=H_{z}^{n-\frac{1}{2}}\left(i+\frac{1}{2},j+\frac{1}{2},k\right)+\frac{2\cdot\Delta t}{\mu\Delta y\cdot\ln(\frac{\Delta y}{r_{0}})} (18)\cdot E_{x}^{n}(i+1/2,j+1/2,k)$$

$$+\frac{\Delta t}{\mu\Delta x}\left[E_{y}^{n}(i,j+1/2,k)-E_{y}^{n}(i+1,j+1/2,k)\right]$$

$$E_{x}^{n+1}(i+1/2,j,k) = \frac{A}{B}E_{x}^{n}(i+1/2,j,k) + \frac{1}{B\Delta y} \begin{bmatrix} H_{z}^{n+\frac{1}{2}}(i+1/2,j+1/2,k) \\ -H_{z}^{n+\frac{1}{2}}(i+1/2,j-1/2,k) \end{bmatrix}$$

$$-\frac{1}{B\Delta z} \begin{bmatrix} H_{z}^{n+\frac{1}{2}}(i+1/2,j,k+1/2) \\ -H_{z}^{n+\frac{1}{2}}(i+1/2,j,k-1/2) \end{bmatrix}$$
(19)

$$A = \frac{(\varepsilon_0 + \varepsilon_s)/2}{\Lambda t} - \frac{\sigma_s/2}{2}$$

$$B = \frac{(\varepsilon_0 + \varepsilon_s)/2}{\Lambda t} + \frac{\sigma_s/2}{2}$$

### II.2. MODELING BY TRANSMISSION LINE THEORY

We begin this part with a brief presentation on the use of line theory for modeling the transient behavior of grounding, and then we present the well-known topological electromagnetic formalism for the analysis of line or cable networks that we adapt for the case of grounding with complex geometry [26].

### **II.2.1 TRANSMISSION LINE EQUATIONS**

The theory of multi-conductor lines (figure .4) is generally derived from Maxwell's equations under certain assumptions. The solutions are posed in the form of waves propagating parallel to the line and with corresponding boundary conditions. Its general equations for a multi-conductor line are [26]:

$$\frac{\partial [i(x,t)]}{\partial x} + [G][v(x,t)] + [C]\frac{\partial [v(x,t)]}{\partial t} = 0$$
 (20)

$$\frac{\partial [v(x,t)]}{\partial x} + [R][i(x,t)] + [L]\frac{\partial [i(x,t)]}{\partial t} = 0$$
 (21)

Where:

[v(x,t)] et [i(x,t)] are the unknown distributed voltage and current along the line, respectively.

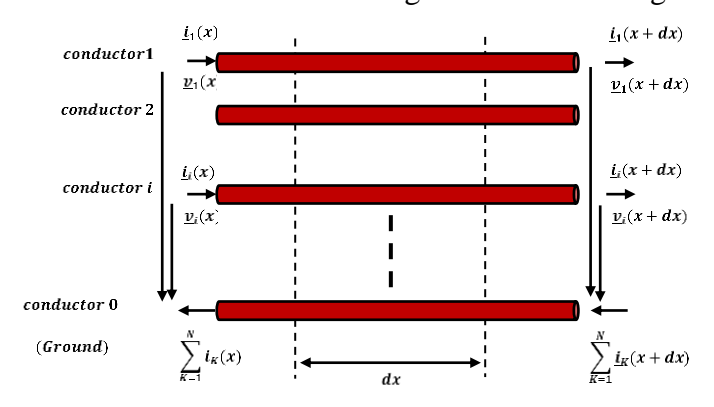


Figure 4:. Infinitesimal section dx of the multi-wire line.

Source: Authors (2025)

The different configurations of grounding systems are composed entirely of conductive wires (electrodes) and are considered as a graph as shown in figure 5. In the presence of an electric wave, each conductor is considered as a single-wire transmission line.

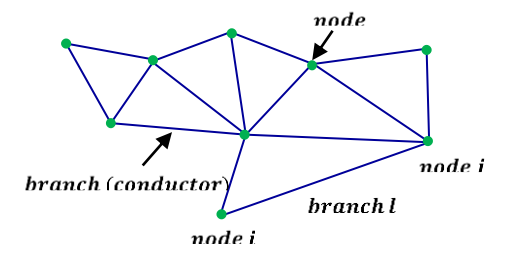


Figure 5: Graph consisting of N transmission lines (branches) and m nodes. Source: Authors (2025)

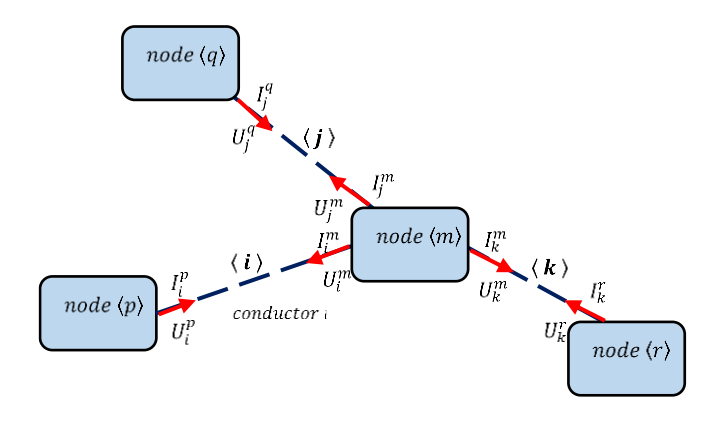


Figure 6: Definition of voltages and currents in a conductor network. Source: Authors (2025)

To solve the problem of the propagation of electric waves in grounding, a matrix system of equations of the type [27]:

$$f(X) = 0 (22)$$

Is required; where equation (22) is represented by the following system of equations:

$$\begin{cases} f_1(x_1, x_2, \dots, x_n) = 0 \\ f_2(x_1, x_2, \dots, x_n) = 0 \\ \vdots \\ f_n(x_1, x_2, \dots, x_n) = 0 \end{cases}$$

$$X = [x_1, x_2, \dots, x_n]^t$$
(23)

Where  $f_i$  represents nonlinear functions of the variables  $x_1, x_2, \dots, x_n$ . The system (22) can be written in the following form [27]:

$$f(X) = [A][X] - [B] = 0 (25)$$

Where the matrix product [A][X] is linear, and [B]=g(X)

With:

$$g(X) = \begin{cases} g_1(x_1, x_2, \dots, x_n) \\ g_2(x_1, x_2, \dots, x_n) \\ \vdots \\ g_n(x_1, x_2, \dots, x_n) \end{cases}$$
(26)

 $g_i$  represents nonlinear functions of the variables  $x_1, x_2, \dots, x_n$ .

In the absence of nonlinearity, the system (III.25) is simplified and can be written in the following form:

$$[A][X] = [B] \tag{27}$$

Where

[X] is the unknown vector of nodal currents and voltages and [B] is the source vector.

### II.2.2 SOLUTION OF TRANSMISSION LINE EQUATIONS

Recall that in frequency the line equations are written as follows for a two-wire line [28]:

$$\frac{\partial V(x,\omega)}{\partial x} + ZI(x,\omega) = 0 \tag{28}$$

$$\frac{\partial V(x,\omega)}{\partial x} + ZI(x,\omega) = 0 \tag{29}$$

Using the matrix [Ø], the general solution of the two equations (28) and (29) is given by [III.14]:

$$\begin{bmatrix} V(x) \\ I(x) \end{bmatrix} = \left[ \phi(x - x_0) \right] \cdot \begin{bmatrix} V(x_0) \\ I(x_0) \end{bmatrix} \tag{30}$$

Where the complex matrix  $[\emptyset(x-x_0)]$  is a state transition matrix and x is an arbitrary point fixed along the branch (electrode) with  $x \ge x_0$  which is expressed in the fractional form for a bifilar line as follows:

$$\begin{bmatrix} V(x) \\ I(x) \end{bmatrix} = \begin{bmatrix} \emptyset_{11}(x - x_0) & \emptyset_{12}(x - x_0) \\ \emptyset_{21}(x - x_0) & \emptyset_{22}(x - x_0) \end{bmatrix} \cdot \begin{bmatrix} V(x_0) \\ I(x_0) \end{bmatrix}$$
(31)

Or else:

$$\begin{bmatrix} V(x) \\ I(x) \end{bmatrix} = [\emptyset] \cdot \begin{bmatrix} V(x_0) \\ I(x_0) \end{bmatrix}$$
 (32)

A partir de (30), aux deux extrémités de la branche de longueur l nous aurons, pour x = let  $x_0 = 0$ , la relation matricielle suivante:

$$[1_{2N}] \cdot \begin{bmatrix} V(l) \\ I(l) \end{bmatrix} - \begin{bmatrix} \emptyset_{11}(l) & \emptyset_{12}(l) \\ \emptyset_{21}(l) & \emptyset_{22}(l) \end{bmatrix} \cdot \begin{bmatrix} V(0) \\ I(0) \end{bmatrix} = \begin{bmatrix} \begin{bmatrix} 0 \\ \end{bmatrix} \end{bmatrix} \quad (32)$$

#### II.2.3. DEVELOPMENT OF THE MATHEMATICAL FORMALISM

To deduce the distribution of currents and voltages in a grounding system, we use the topological formalism which consists of solving a set of propagation equations (for all the branches constituting the grounding network) taking into account the electrical relations at the ends of each branch (electrode). Very schematically for a grounding network with n nodes, we must construct a system of linear equations having the following form [29]:

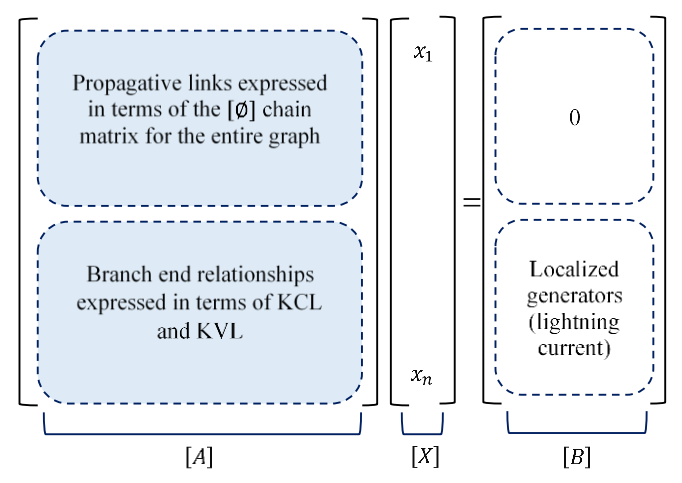


Figure 7: Topological formalism Source: Authors (2025)

### With:

[A1]: submatrix deduced from the matrix representation Ø of the branches (electrodes);

[A2]: submatrix deduced from Kirchhoff's laws (KCLet KVL) for the graph (end and interconnection network);

[X]: the unknown vector, contains the nodal currents and voltages on all the nodes of the network.

[B]: the excitation vector.

### II.3. CST SOFTWARE

Generally speaking, the sequence of CST software based on Finite Integration Technique [30], equipped with an interface schematized by figure.8

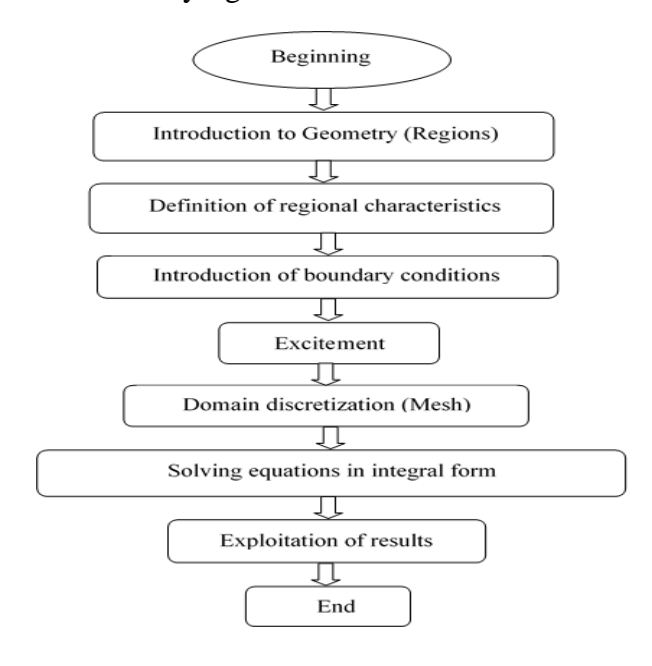


Figure 8: Flowchart of the different modules of the CST software Source: Authors (2025)

#### III. APPLICATION

Earthing plays a very important role in disturbed conditions in electrical networks. It is therefore essential to have a good understanding of its transient behavior, especially during a storm discharge. Although measurement is possible in an industrial environment, it remains expensive and, above all, insufficient to address all of the engineer's concerns. For more than two decades now, specialists in electrical network protection have been using simulation software to try to answer the many questions of insulation coordination, rapid evacuation of the high electrical charge that appears during a short circuit or a storm discharge, and the organization of earth networks. In this section, we focus on applications dedicated to modeling the transient behavior of earthing. The objective of these different applications is to highlight the possibilities offered by realistic modeling (simple mathematical model, low calculation time and acceptable accuracy) based on the concept of transmission lines and analytical expressions deduced from the measurement. To support our simulation results, we compare them with those obtained by performing modeling by analytical approach (TL- matrix[Ø]) where we use the numerical resolution of Maxwell's equations by FDTD as well the finite integration Technique (CST Software).

#### III.1.VALIDATIONS

To validate our modeling of the transient behavior of an earth connection based on line theory using the TL- matrix  $[\emptyset]$ , FIT in CST Software or by FDTD (FDTD), we propose to treat a simple horizontal electrode then a real-dimensional earthing grid equipping an overhead station, electrode buried horizontally in a homogeneous ground

For this first application, it is an electrode (figure 9) of length l, buried horizontally at a depth h in a ground defined by its physical characteristics ( $\epsilon$ ,  $\mu$  and  $\rho$ ) and supplied by a bi-exponential current source. The application data are summarized in Table .1

	• $i(t) = I_0(\exp(-\alpha t) - \exp(-\beta t))$
Lightning wave	• $I_0 = 30 \ KA$
generator	• $\alpha = 45099 \mu s^{-1}$
	• $\beta = 9022879 \mu s^{-1}$
	l = 20 m
Electrode	$\bullet  \emptyset = 14 \ mm$
	$\bullet  h = 0.4  m$
	• $\varepsilon_r = 36$
Ground	• $\mu_r = 1$

Table 1: Characteristic electrode buried horizontally Source: Authors (2025)

Figure 9: Electrode buried horizontally. Source: Authors (2025)

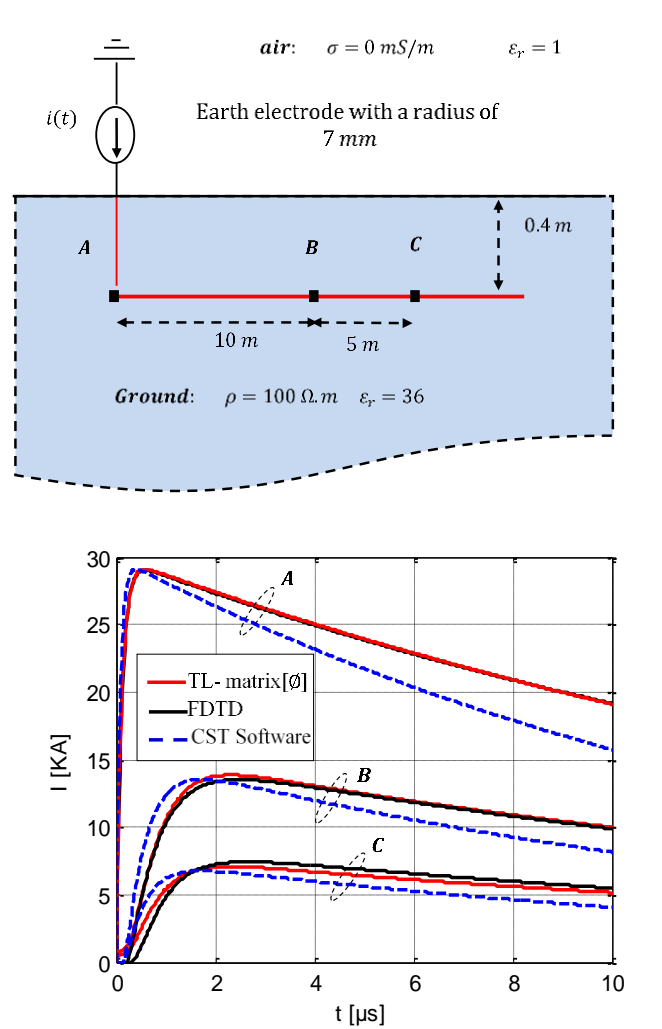


Figure 10: Current variation at different points of the electrode. Source: Authors (2025)

In Figure .10, we have the results for the variation of the longitudinal current at different points (A, B and C) of the electrode (figure .8) that we obtain by the FDTD, analytical approach by TL – matrix [Ø] and those carried out using the CST software. The analysis of these results highlights a conservation of the general shape and amplitude for the three models, but with a very slight time shift between those obtained directly in the time domain FDTD and those carried out after application of IFFT; this shift is the result of the time-frequency passage and vice versa using the Fourier transform.

Good agreements are found between the results obtained by TL- matrix  $[\emptyset]$  and those obtained by the FDTD and FIT method under the CST software.

### **III.2. GROUNDING GRID**

We treat a grounding grid, equipping an overhead station, of real dimensions ( $60m \times 60m$ ) shown in figure.11

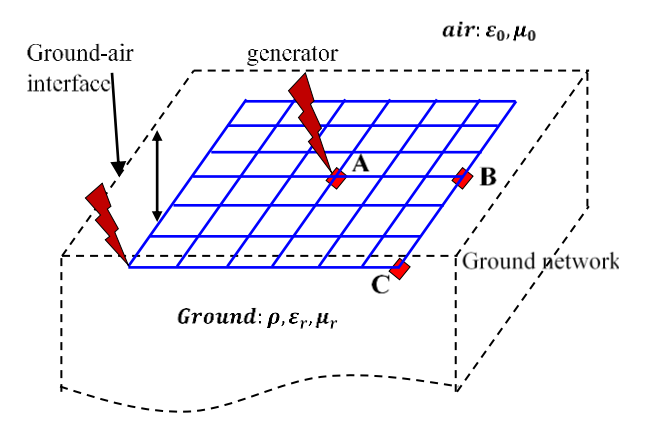


Figure 11: Grounding grid. Source: Authors (2025)

Table .2 summarizes all the data for this application.

	• $i(t) = I_0(\exp(-\alpha t) - \exp(-\beta t))$
Lightning wave	$I_0 = 1.2  KA$
generator 1	$\alpha = 0.0142 \mu s^{-1}$
	$\beta = 1.073  \mu s^{-1}$
	• $i(t) = I_0(\exp(-\alpha t) - \exp(-\beta t))$
Lightning wave	$I_0 = 1.0167  KA$
generator 2	$\alpha = 0.0142 \mu s^{-1}$
	• $\beta = 5.073 \mu s^{-1}$
	l = 60 m
Electrode	$\bullet$ Ø = 14 mm
	$\bullet  h = 0.5  m$
	• $\varepsilon_r = 36$
Ground	$\mu_r = 1$

Table 2: Characteristic lightning wave in the middle of the grid Source: Authors (2025)

We examine the injection of a lightning wave into the middle of the grid as shown in figure 11.

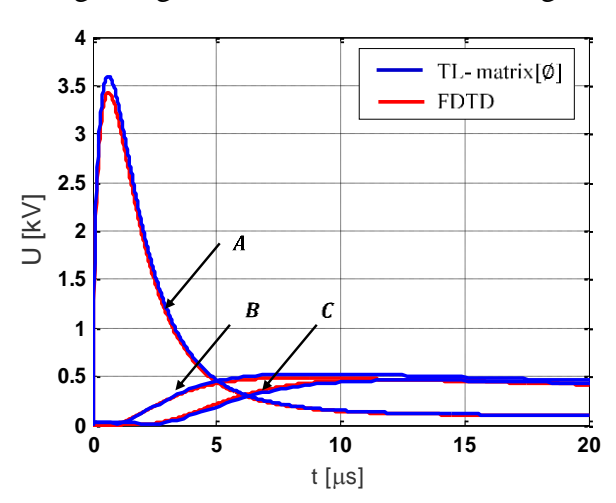


Figure 12: Temporal variation of the potential at points A, B and C (our calculations). Source: Authors (2025)

In Figure 12 we have the temporal variation of the potential at different points of the grid (figure 10), obtained successively by the numerical method and the analytical method. The concordance of the results is excellent in shape and amplitude; we note that the effect of the frequency only occurs at the beginning of the transient and is manifested by a difference in amplitude. The calculations by the TL-matrix[ $\emptyset$ ] and by the FDTD lead to almost identical results; the big difference is in terms of calculation time. If the two formalisms lead to comparable results in terms of precision.

### III.3 STRATIFIED GROUND WITH TWO HORIZONTAL LAYERS

To deal with the case of a buried earthing in a stratified ground, it is clear that the resolution of Maxwell's equations in continuous media remains the most appropriate and rigorous means; this modeling must take into account the open boundaries (air and ground) and the different interfaces (ground-air and ground-ground). In the literature some works [31] devoted to the radiation of an antenna buried in a stratified ground are proposed for the calculation of the field when the antenna and the observation point are located in the same medium. This modeling requires a modification of the Green's Dyadic kernel and remains very heavy from a mathematical point of view [31]. In order to simplify this modeling, in our research work, we propose in the direct resolution by FDTD of Maxwell's equations taking into account the stratification of the ground. Also, to judge the quality of the results achieved for laminated ground using the FDTD and TL-matrix [\varphi], we use the concept of apparent resistivity applicable in the case of a two-layer ground [32]. For all applications, relating to laminated ground, we use a voltage generator to simplify the implementation of the formalism which consists in solving Maxwell's equations by FDTD. The choice of this type of generator will allow us to directly confront the simulation results.

### III.3.1. APPARENT RESISTIVITY OF A TWO-LAYER GROUND

A two-layer ground can be represented by an upper layer of finite depth above a lower layer of infinite depth (figure 13). The abrupt change in resistivity at the interface between the two soil layers can be described by means of a reflection factor K [32] defined by

$$K = \frac{\rho_2 - \rho_1}{\rho_2 + \rho_1} \tag{33}$$

Where:

 $\rho_1$  and  $\rho_2$  are the electrical resistivity of the upper and lower layers, respectively, as shown in the following figure:

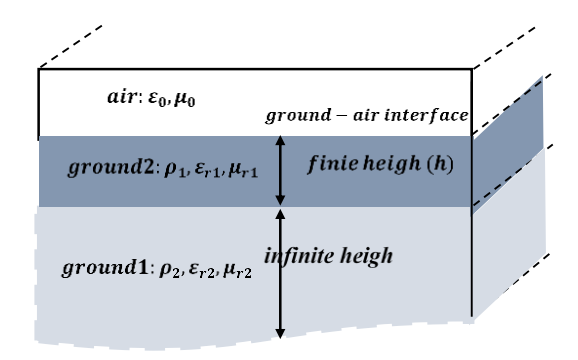


Figure 13: Two-layer laminate flooring. Source: Authors (2025)

In order to take into account ground stratification in our present line theory approach, we use an expression derived from Wenner's method [32] which gives an apparent resistivity of a ground consisting of two horizontally stratified layers (figure 13). In terms of the parameters shown in figure 12 above the apparent resistivity  $\rho_a$  of the stratified ground is given as follows:

$$\rho_a = \rho_1 \left[ 1 + 4 \sum_{n=1}^{\infty} \frac{K^n}{\sqrt{1 + \left(2n\frac{h}{a}\right)^2}} - \frac{K^n}{\sqrt{4 + \left(2n\frac{h}{a}\right)^2}} \right]$$
(34)

# III.3.2. ELECTRODE BURIED HORIZONTALLY IN A TWO-LAYER GROUND

Figure 14 shows an electrode of length l buried horizontally at a depth h in a two-layer ground. The electrode is excited by a voltage source given by a double-exponential function. Table 3 below summarizes the physical and geometric data of this application.

	$ v(t) = V_0(\exp(-\alpha t) - \exp(-\beta t)) $
Lightning wave	• $V_0 = 30  KV$
generator	• $\alpha = 45099  \mu s$
	• $\beta = 9022879 \mu s$
Electrode	l = 20 m
	$\bullet  \emptyset = 14 \ mm$
	$\bullet  h = 0.4 \ m$
Top layer	• $\varepsilon_r = 36$
	$\mu_r = 1$
	• $h_{superieure} = 2 m$
Lower layer	• $\varepsilon_r = 36$
	$\mu_r = 1$
	$\bullet  h_{inferieure} = \infty m$

Table 3: Characteristic lightning wave in a two layer grid Source: Authors (2025)

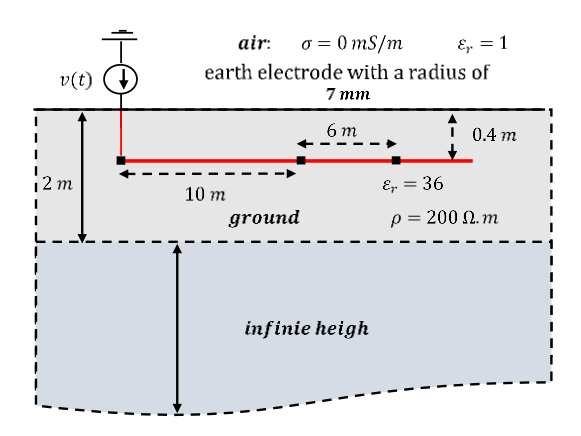


Figure 14: Electrode buried horizontally in a two-layer ground. Source: Authors (2025)

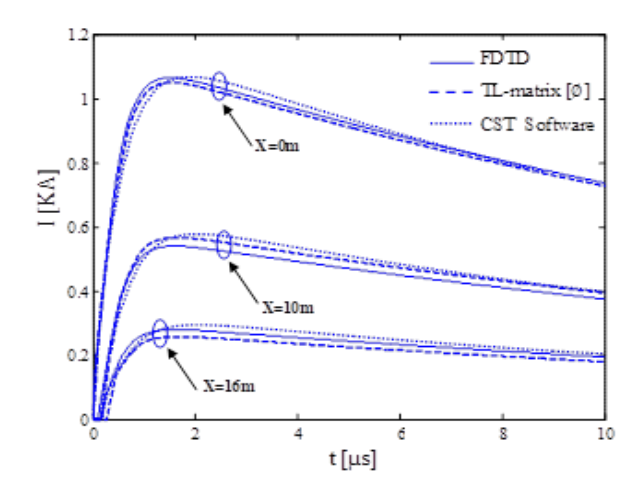


Figure 15: Temporal variation of the current at different points of the electrode (0, 10 and 16 m). Source: Authors (2025)

In Figure 15 we have the current at different points of the buried electrode obtained by three different models; we can notice that the three approaches provide comparable results both in amplitude and in general appearance. The concept of apparent resistivity is approved by the direct numerical resolution of Maxwell's equations by FDTD for a stratified ground.

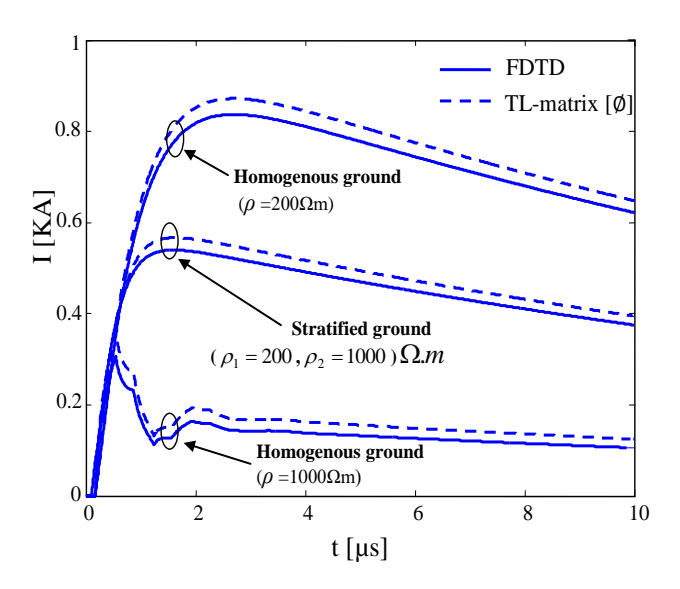


Figure 16: Temporal variation of the current in the middle of the electrode. Source: Authors (2025)

Figure 16 illustrates the temporal variation of the current in the middle of the electrode for a homogeneous ground ( $\rho$ =200  $\Omega$ m, then  $\rho$ =1000  $\Omega$ m) and a stratified ground ( $\rho$ 1=200  $\Omega$ m and  $\rho$ 2=1000  $\Omega$ m). We note that the current in the earth conductor (electrode) is indeed a function of the charge (ground resistivity).

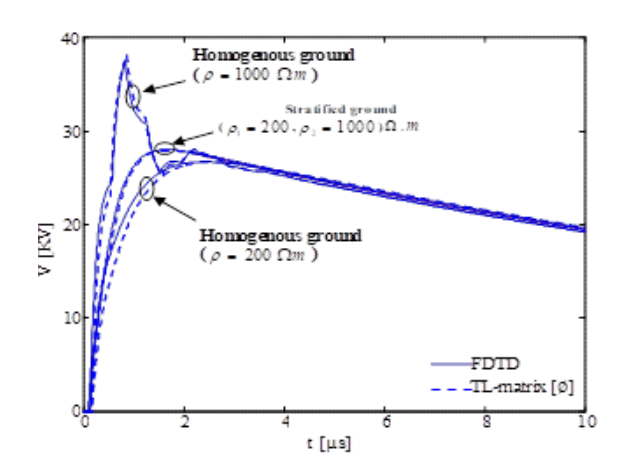


Figure 17: Temporal variation of the voltage in the middle of the electrode. Source: Authors (2025)

#### VI. CONCLUSION

The problem of earthing is very old and still topical, given its interest in protecting equipment and electrical devices. This particular interest has seen the emergence of various measurement methods and especially mathematical, analytical, semi-analytical and numerical models to analyze the behavior of a ground grab. These methods are developed from the laws of electromagnetism or general equations of transmission lines.

In this work, we propose a realistic modeling able to respond to the concerns of engineers, taking into account the above-mentioned indicators. For this purpose we based our study on the use of topological electromagnetic formalism using the concept of TL-matrix  $[\emptyset]$ , FDTD and CST Software. Indeed, given the filliform nature of the conductors that intervene in the realization of an earthing we considered it advantageous to use the concept of lines as well in frequency as in time.

The different analytical and numerical methods used, both in frequency and time, we are able to respond adequately to the request of engineers who need to carry out very advanced parametric studies for a better knowledge of the desired grounding.

#### V. AUTHOR'S CONTRIBUTION

**Conceptualization:** Mohammed Kaouka, Hakim Azizi, Adelhadi Hameurlaine, Daoud Sekki, Mohammed chebout, Mohammed Charif Kihal and Marouane Kihal

**Methodology:** Mohammed Kaouka, Hakim Azizi, Adelhadi Hameurlaine, Mohammed chebout, Daoud Sekki **Investigation:** Mohammed Kaouka, Hakim Azizi, Mohammed chebout, Daoud Sekki, and Mohammed Charif Kihal

Discussion of results: Hakim Azizi, Mohammed Charif Kihal

**Writing – Original Draft:** Hakim Azizi, Adelhadi Hameurlaine, Daoud Sekki, Mohammed chebout, Mohammed Charif Kihal and Marouane Kihal

Writing – Review and Editing: Hakim Azizi, Adelhadi Hameurlaine, Mohammed Charif Kihal, Marouane Kihal and Daoud Sekki

Resources: Mohammed Kaouka, Hakim Azizi, Daoud Sekki, Mohammed chebout and Mohammed Charif Kihal

Supervision: Hakim Azizi, Adelhadi Hameurlaine, Mohammed Charif Kihal and Marouane Kihal

Approval of the final text: Hakim Azizi, Mohammed Charif Kihal, Daoud Sekki and Mohammed chebout,

### VI. ACKNOWLEDGMENTS

The authors of this article would like to thank the General Directorate of Scientific Research and Technological Development (DGRSDT) in Algeria for their technical support and the specific research budget allocated to this program.

#### VII. REFERENCES

- [1] Gabriel A. Adegboyega, Kehindo O. Odeyemi. Assessment of Soil Resistivity on Grounding of Electrical Systems: A Case Study of North-East Zone, Nigeria. Journal of Academic and Applied Studies Vol. 1(3) September 2011.pp28-38. Available online:www.academians.org
- [2] Prasad Dwarka, Sharma H.C. Soil Resistivity and Earthing System. International Journal of Management, IT and Engineering, 2012 September; Volume2, Issue9
- [3] Omar, K., Sofiane, C., Madjid, T., et al.: Time-domain modelling of grounding systems impulse response incorporating nonlinear. IEEE Trans. Electromagn. Compat. 60(4), 1–9 (2017)
- [4] Leonid, G.: Time and frequency-dependent lightning surge characteristics of grounding electrodes. IEEE Trans. Power Delivery 24(4), 2186–2196 (2009)
- [5] Gouda, O.E., Dein, A.Z.E., Omar, S.Y., Lehtonen, M., et al.: Studying direct lightning stroke impact on human safety near HVTL towers consid-ering two layer soils and ionization influence. IEEE Access 11, 5019–5030 (2023)
- [6] de Araújo, A.R.J., Colqui, J.S.L., et al.: Computation of ground potential rise and grounding impedance of simple arrangement of electrodes buried in frequency-dependent stratified soil. Electr. Power Syst. Res. 198, 107364 (2021)
- [7] Zeng, R., Gong, X., He, J., et al.: Lightning impulse performances of grounding grids for substations considering soil ionization. IEEE Trans. Power Delivery 23(2), 667–675 (2008)
- [8] Sengar, K.P., Chandrasekaran, K.: Transient analysis of earthing electrodes considering soil ionization phenomenon under lightning impulse condition. Electr. Eng. 106, 3083–3096 (2023)
- [9] Lima, A.C.S., Vieira, P.H., Schroeder, M.A.O., Moura, R.A.R.: Modeling grounding systems for electromagnetic compatibility analysis. Recent Topics in Electromagnetic Compatibility, pp. 81–101. IntechOpen, UK (2022)
- [10] Mokhtari, M., Abdul-Malek, Z., Wooi, C.L.: Integration of frequency dependent soil electrical properties in grounding electrode circuit model. Int. J. Electr. Comput. Eng. 6(2), 792 (2016)
- [11] Stoll, R.L., Chen, G., Pilling, N.: Comparison of two simple high-frequency earthing electrodes. IEE Proc. Gener. Transm. Distrib. 151(2), 219–224 (2004
- [12] Mestriner, D., Antônio Ribeiro de Moura, R., Procopio, R., et al.: Impact of grounding modeling on lightning-induced voltages evaluation in distribution lines. Appl. Sci. 11(7), 2931 (2021). https://doi.org/10.3390/
- [13] Gouda, O.E., et al.: Performance of grounding electrodes under lightning strokes in uniform and two-layer soils considering soil ionization. IEEE Access 10, 76855–76869 (2022)
- [14] Farina, L., Mestriner, D., Procopio, R., et al.: The lightning power electro-magnetic simulator for transient over voltages (LIGHT-PESTO) code: A user-friendly interface with the Matlab-Simulink environment. IEEE Lett. Electromagn. Compat. Pract. Appl. 2(4), 119–123 (2020)
- [15] R. Verma and D. Mukhedkar, "Impulse to impedance of buried ground wires", IEEE Transactions on Power Apparatus and Systems, Vol. PAS-99, No. 5, pp. 2003-2007, Sep./Oct., 1980.

- [16] L. Greev and F. Dawalibi, "An electromagnetic model for transients in grounding system", IEEE Trans. Power Delivery, Vol. 5, pp. 1773-1781, November 1990.
- [17] Alipio, R., Coelho, V.L., Canever, G.L.: Experimental analysis of horizontal grounding wires buried in high-resistivity soils subjected to impulse currents. Electr. Power Syst. Res. 214, 108761 (2023)
- [18] Ala, G., Viola, F., Buccheri, P.L., Romano, P.: Finite difference time domain simulation of Earth electrodes soil ionisation under lightning surge condition. IET Sci. Meas. Technol. 2(3), 134–145 (2008)
- [19] **K. Otani and al.**, "FDTD Simulation of Grounding Electrodes Considering Soil Ionization"; International Conference on Lightning Protection (ICLP), IEEE Symposium- Vienna, Austria . 2012
- [20] Omar, K., Sofiane, C., Madjid, T., et al.: Time-domain modeling of grounding systems' impulse response incorporating nonlinear and frequency-dependent aspects. IEEE Trans. Electromagn. Compat. 60(4), 907–916 (2018)
- [21] **K. Otani and al.**, "FDTD Simulation of Grounding Electrodes Considering Soil Ionization"; International Conference on Lightning Protection (ICLP), IEEE Symposium- Vienna, Austria . 2012
- [22] **A. Taflove, K. R. Umshankar and K. S. Yee,** Detailed FDTD Analysis of Electromagnetic Fields Penetration Narrow Slots and Lapped Joints in Thick Conducting Screens », IEEE Trans. Antennas and Propagation, Vol. 36, n° 2, pp. 247-257, Feb. 1988.
- [23] Yee, K. S. (1966). Numerical solution of initial boundary value problems involving Maxwell's Equations in isotropic media. *IEEE Trans. Antennas and propagation*, no. 14, pp. 302-307.
- [24] R.S. Alípio, M. A. O. Schroeder, M. M. Afonso, T A.S. Oliveira, "Electrical fields of grounding electrodes with frequency dependent soil parameters", Electric Power Systems Research 83, pp. 220–226, 2012.
- [25] **K. Tanabe, A. Asakawa,** « Computer Analysis of transient Performance of Grounding Grid Element Based on the Finite-Difference Time-Domaine Method», CongrésInternational IEEE-EMC 2003, Istanbul-Turque, 11-16 Mai 2003.
- [26] C.R. Paul, "Analysis of multiconductor transmission lines", John Wiley and Sons, Inc., New York, 1984.
- [27] Brignone, M., Procopio, R., Mestriner, D., et al.: Analytical expressions for lightning electromagnetic fields with arbitrary channel-base current—part I: Theory. IEEE Trans. Electromagn. Compat. 63(2), 525–533 (2020)
- [28] Mestriner, D., Brignone, M., Procopio, R., Rossi, M., et al.: Analytical expressions for lightning electromagnetic fields with arbitrary channel-base current. Part II: Validation and computational performance. IEEE Trans. Electromagn. Compat. 63(2), 534–541 (2020)
- [29] Gouda, O.E., Dein, A.Z.E., Tag-Eldin, E., et al.: Proposed approach to investigate the current and voltage distributions of isolated and grounded systems during earth fault conditions. IEEE Access 11, 98362–98375 (2023)
- [30] Korecki, J., Le Menach, Y., Ducreux, J-P., Piriou, F. (2008). Numerical solutions in primal and dual mesh of magnetostatic problem solved with the Finite Integration Technique. *COMPEL*, no.1, pp. 47-

- [31] **V.Arnautovski-Toseva, L. Grcev**," Electromagnetic analysis of horizontal wire in two-layered soil", Elsevier, Journal of Computational and Applied Mathematics, Vol 168, pp 21-29,2004.
- [32] Research Project of PEA's Ground Grid in Substation and Grounding in HV and LV Distribution System, Thailand, 2006